

Wind measurements with 355-nm molecular Doppler lidar

Bruce M. Gentry

Laboratory for Atmospheres, Code 912, NASA Goddard Space Flight Center, Greenbelt, Maryland 20771

Huailin Chen

Science and Engineering Services, Inc., Burtonsville, Maryland 20866

Steven X. Li

Orbital Sciences Corporation, Greenbelt, Maryland 20770

Received April 27, 2000

A Doppler lidar system based on the molecular double-edge technique is described. The system is mounted in a modified van to permit deployment in field operations. The lidar operates with a tripled Nd:YAG laser at 355 nm, a 45-cm-aperture telescope, and a matching azimuth-over-elevation scanner to permit full sky access. Validated atmospheric wind profiles were measured from 1.8 to 35 km with a 178-m vertical resolution. The range-dependent rms deviation of the horizontal wind speed is 0.4–6 m/s. The measured wind speed and direction are in good agreement with the rawinsonde wind measurements made simultaneously from the same location. © 2000 Optical Society of America

OCIS codes: 010.3640, 120.2230, 010.7030, 120.0280.

Research has established the importance of global tropospheric wind measurements for large-scale improvements in numerical weather prediction.¹ In addition, wind measurements from ground and airborne platforms provide data that are fundamental to the understanding of mesoscale dynamic processes, transport, and exchange in the atmosphere.

A mobile lidar system that uses direct-detection Doppler lidar techniques for measuring wind profiles was recently completed at the NASA/Goddard Space Flight Center. The variety of direct-detection Doppler wind lidar measurements that were recently reported indicate the growing interest in this area.^{2–6} The wind lidar program at Goddard has concentrated on the implementation of the direct-detection Doppler lidar using the edge technique.⁷ The basic principles of the edge technique have been verified in laboratory⁸ and atmospheric³ lidar wind experiments.

The double-edge technique was developed to extend the wind measurement capability into the troposphere and the lower stratosphere. Details of the double-edge method were recently reported for lidar systems to measure the Doppler shift from either aerosol⁹ or molecular¹⁰ backscatter signals. Atmospheric measurements of winds by aerosol implementation of the double-edge technique have also been reported.¹¹

In this Letter we describe a double-edge molecular Doppler lidar system that operates at 355 nm and present the results of measurements of horizontal wind speed and direction made at Goddard (38:59:32N, 76:51:10W). The lidar measurements are compared with rawinsonde wind measurements taken simultaneously from the same location.

The molecular double-edge technique uses two edge filters located in the wings of the thermally broadened molecular backscattered signal spectrum at 355 nm to determine the velocity of the wind. This arrangement is shown in Fig. 1. The two edge filter bandpasses, labeled Edge1 and Edge2, are shown, along with the atmospheric backscattered spectrum. The atmospheric

backscatter spectrum shows the characteristic narrow spike from aerosols along with the thermally broadened molecular spectrum. A Doppler shift in the outgoing laser frequency is observed that is proportional to the component of the wind velocity along the line of sight of the laser beam. Because of the symmetric arrangement of the filters about the laser frequency, the Doppler shift will cause the transmitted signal to increase in one edge filter and to decrease in the other one. The ratio of the two edge-channel signals is sensitive to the wind's speed and direction and provides a unique measure of them. The wavelength of operation is chosen to be in the ultraviolet to take advantage of the λ^{-4} dependence of the molecular backscatter. A third etalon channel, labeled Locking Filter in Fig. 1, is used to monitor the outgoing laser frequency to remove inaccuracies that are due to the frequency drift of the laser or the etalon.

The optical layout of the lidar system is shown in Fig. 2. The transmitter is an injection-seeded

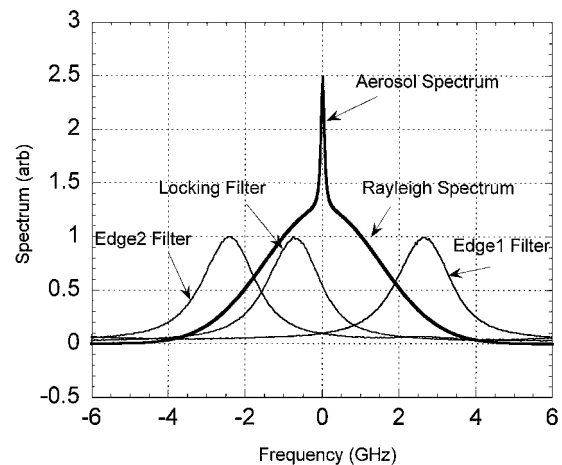


Fig. 1. Spectra of the atmospheric backscattered Rayleigh and aerosol signals along with three etalon transmission functions.

Nd:YAG laser that produces 15-ns pulses at a 10-Hz repetition rate. The energy per pulse at the tripled wavelength of 355 nm is 70 mJ. The spectral linewidth of the laser is ~ 80 MHz, much smaller than the spectral width of either the atmospheric signal (3.5 GHz) or the edge filters (1.7 GHz). The receiving optical system consists of a 45-cm-aperture telescope and a matching azimuth-over-elevation scanner. The collected signal is focused into a 200- μm fiber-optic cable to couple the signal from the telescope to the receiving box.

Light from the fiber is collimated and split by beam splitters into five beams. Two of the beams are energy monitors: One has a photon-counting photomultiplier (PMT) and the other, an analog mode PMT. The remaining three collimated beams are directed along parallel paths through a Fabry–Perot etalon that is used to measure the frequency shift. The etalon has three subapertures that correspond to the filter bandpass functions labeled Edge1, Edge2, and Locking Channel in Fig. 1. The channels have nearly identical optical properties (peak transmission, finesse, and free spectral range) with slightly different bandpass center frequencies. We created the offset in the bandpass frequency by depositing small step coatings upon one of the plates before applying the reflective coating. This method is similar to that employed by Chanin *et al.*² The separation of the two edge filters is chosen to be 5.1 GHz, so the sensitivity of the broader molecular signal is equal to that of the narrower aerosol signal.¹⁰ The locking etalon peak is located 1.7 GHz from the Edge1 filter peak, so the crossover point of the two edge-filter bandpasses is aligned to the half-height point of the locking filter bandpass. Actively locking the laser and the etalon at this point on the locking filter ensures symmetry of the edge-filter channels for wind measurement. We accomplish the locking by sampling a small portion of the transmitted laser energy to make a reference measurement of the outgoing frequency. The reference signal transmitted through the locking channel etalon is detected by a PMT operating in analog mode and sampled by a boxcar integrator. The boxcar reference measurement is stored to provide correction for short-term frequency jitter and is also used to lock the etalon (all three channels together) to the laser frequency. The atmospheric backscattered light transmitted through the edge-filter etalon channels are detected by PMT's operating in photon-counting mode. The experimental parameters of the 355-nm molecular lidar system are listed in Table 1.

An intercomparison experiment was held on the evenings of November 16 and 17, 1999. The lidar was operated in several modes during the experiment, and correlative measurements of wind speed and direction were obtained from a portable rawinsonde system that was brought to Goddard and operated by personnel from Wallops Flight Facility, Wallops Island, Virginia.

Because of the dynamic range limitations of the photon-counting detectors, two sets of measurements were obtained for the altitude range from 1.8 to 35 km. We made the first set of wind measurements from 1909 to 2047 EST on November 17, 1999, at

a reduced energy of 0.4-mJ/pulse, to determine the lower-altitude wind from 1.8 to 7 km. We made the second set of measurements from 2105 EST on November 17 to 0124 EST on November 18, 1999, at full power (~ 70 mJ/pulse) to measure the wind from 7 to 35 km. We obtained vector wind data by rotating the scanner to measure line-of-sight wind profiles at four azimuth angles with a fixed elevation angle of 45° . The photocounts in each of the three photon-counting detector channels are binned with 250-m range resolution and integrated for 300 shots at each line of sight. Rawinsonde balloons were launched during the course of the evening to provide simultaneous wind profiles for comparison with the lidar.

The horizontal wind field is determined from the ratio of the edge-filter signals determined for each of the four lines of sight. The ratios taken at azimuth angles 180° apart from one another are paired in the analysis to yield two orthogonal components of the horizontal wind field.

Let $r_+(v_{\text{LOS}}) = I_1 + (v_{\text{LOS}})/I_2 + (v_{\text{LOS}})$ and $r_-(-v_{\text{LOS}}) = I_1 - (-v_{\text{LOS}})/I_2(-v_{\text{LOS}})$, where $I_{1,2}$ refer to the signals received through filters Edge1 and Edge2, pluses and minuses represent the two lines of sight measured for each component, and v_{LOS} is the line-of-sight wind velocity for a given component. The atmosphere is assumed to be spatially uniform during the time of integration.

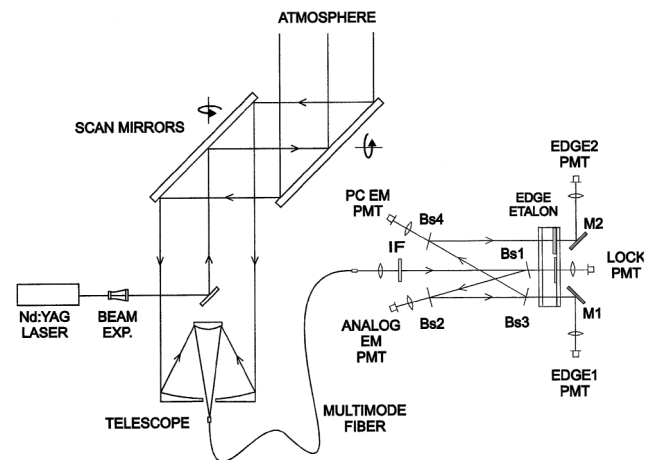


Fig. 2. Optical diagram of the 355-nm molecular wind lidar system: BS1–BS4, beam splitters; EM, energy monitor; PC, photon-counting; M1, M2, mirrors; IF, interference filter; EXP, beam expander.

Table 1. Molecular Doppler Lidar System Parameters

Wavelength	355 nm
Telescope–scanner aperture	0.45 m
Laser linewidth (FWHH)	80 MHz
Laser energy/pulse	70 mJ
Etalon free spectral range	12 GHz
Etalon FWHH	1.7 GHz
Edge channel separation	5.1 GHz
Locking channel separation	1.7 GHz
Etalon peak transmission	>60%
PMT quantum efficiency	25%

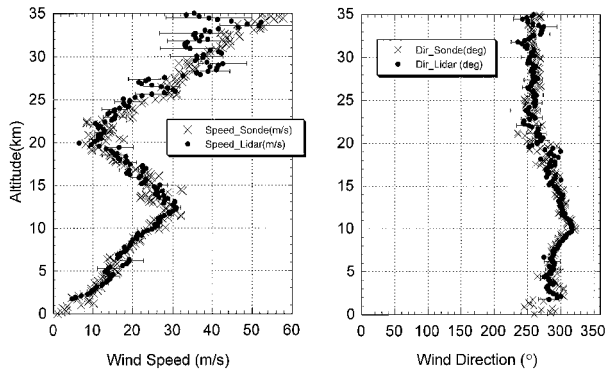


Fig. 3. Profiles of wind speed and direction measured by the molecular lidar system compared with data from a collocated balloon sonde on November 17, 1999.

We now define the sensitivity θ to be the fractional change in the measured ratio r for a given velocity:

$$\theta = \frac{\partial r}{r \partial \mathbf{v}} = \frac{\partial I_1}{I_1 \partial \mathbf{v}} - \frac{\partial I_2}{I_2 \partial \mathbf{v}}. \quad (1)$$

The sensitivity is determined by the spectral characteristics of the two edge filters, which can be measured in calibration scans (see Fig. 1), and by the spectral properties of the atmospheric backscattered return. As noted above, the aerosol and the molecular components of the backscattered signal have different spectral characteristics. The offset between the two filters is chosen to have equal sensitivity to molecular and aerosol signals. The approximate value of θ for our system for small Doppler shifts is 0.0065 (m/s). The velocity component is now given by

$$\mathbf{v}_{\text{LOS}} = \frac{r_+(\mathbf{v}) - r_-(-\mathbf{v})}{[r_+(\mathbf{v}) + r_-(-\mathbf{v})]} \frac{1}{\theta}. \quad (2)$$

The horizontal wind speed and direction are determined from the two orthogonal line-of-sight wind velocities.

Figure 3 shows a summary of the comparison of wind speed and direction. Filled circles represent the lidar measured results along with error bars. The crosses are the sonde measurement results. Thirty scan cycles were averaged for low-altitude measurement from 1.8 to 7 km with a vertical resolution of 178 m. Wind errors ranged from 0.6 m/s at 1.8 km to 4 m/s at 7 km.

The high-altitude wind speeds and directions from 7 to 35 km were determined from the average of 80 scan cycles. The mean wind speed and the resultant error bars are given for 178-m vertical resolution from 7 to 25 km. Wind errors in this region are 0.4 m/s at

7 km, 0.7 m/s at 10 km, 1.8 m/s at 15 km, and 3.9 m/s at 20 km. For altitudes above 25 km the vertical resolution is 707 m and the observed errors are 6.5 m/s at 30 km.

The lidar measurements are in good agreement with the balloon results. The wind profiles of both the lidar and the rawinsonde show clear evidence of a mid-level jet at 12.5 km with a local maximum speed of 30 m/s. A second higher-level jet was observed with a speed of nearly 50 m/s at 35 km. A local minimum of 12 m/s in the wind speed was observed at 21 km.

In conclusion, we have developed and successfully demonstrated operation of a 355-nm Doppler wind lidar system based on the double-edge technique. Lidar measured profiles of wind speed and direction were obtained to altitudes of as much as 35 km. The lidar measurements and the independent rawinsonde wind measurements are in very good agreement.

This research was supported in part by the NASA Earth Science Enterprise Office (Research and Technology Objective and Plans Summary 622-01-01) and the National Polar-Orbiting Operational Environmental Satellite Integrated Program Office. The development of the receiver was supported by the NASA New Millennium program. The authors acknowledge the efforts of the Zephyr Doppler lidar engineering team, particularly Mike Pryzby and Vince Canali of Swales Aerospace and Mark Neuman and Randy Pensabene of Orbital Sciences Corporation. B. M. Gentry's e-mail address is bruce.gentry@gsfc.nasa.gov.

References

1. W. Baker, G. D. Emmitt, F. Robertson, R. Atlas, J. Molinari, D. Bowdle, J. Paegle, R. M. Hardesty, R. Menzies, T. Krishnamurti, R. Brown, M. J. Post, J. Anderson, A. Lorenc, and J. McElroy, *Bull. Am. Meteorol. Soc.* **76**, 869 (1995).
2. M. L. Chanin, A. Garnier, A. Hauchecorne, and J. Porteneuve, *Geophys. Res. Lett.* **16**, 1273 (1989).
3. C. L. Korb, B. M. Gentry, and S. X. Li, *Appl. Opt.* **36**, 5976 (1997).
4. M. J. McGill, W. R. Skinner, and T. D. Irgang, *Appl. Opt.* **36**, 1928 (1997).
5. J. S. Friedman, C. Tepley, P. Castleberg, and H. Roe, *Opt. Lett.* **22**, 1648 (1997).
6. C. Souprayen, A. Garnier, A. Hertzog, A. Hauchecorne, and J. Porteneuve, *Appl. Opt.* **38**, 2410 (1999).
7. C. L. Korb, B. M. Gentry, and C. Y. Weng, *Appl. Opt.* **31**, 4202 (1992).
8. B. Gentry and C. L. Korb, *Appl. Opt.* **33**, 5770 (1994).
9. C. L. Korb, B. M. Gentry, S. X. Li, and C. Flesia, *Appl. Opt.* **37**, 3097 (1998).
10. C. Flesia and C. L. Korb, *Appl. Opt.* **38**, 432 (1999).
11. B. Gentry, S. Li, C. L. Korb, S. Mathur, and H. Chen, in *Proceedings of the 19th International Laser Radar Conference*, NASA CP-1998-207671 (NASA, Washington, D.C., 1998), p. 587.